

AperTO - Archivio Istituzionale Open Access dell'Università di Torino

The Meso-Cenozoic stratigraphic succession of the Col de Braus area (Maritime Alps, SE France)

This is the author's manuscript

Original Citation:

Availability:

This version is available <http://hdl.handle.net/2318/1542757> since 2016-11-29T11:09:12Z

Published version:

DOI:10.1080/17445647.2015.1077167

Terms of use:

Open Access

Anyone can freely access the full text of works made available as "Open Access". Works made available under a Creative Commons license can be used according to the terms and conditions of said license. Use of all other works requires consent of the right holder (author or publisher) if not exempted from copyright protection by the applicable law.

(Article begins on next page)



UNIVERSITÀ DEGLI STUDI DI TORINO

This is an author version of the contribution published on:

Questa è la versione dell'autore dell'opera:

Journal of Maps, 2015, DOI: 10.1080/17445647.2015.1077167

ovvero Barale et al., Taylor & Francis, 2015, pagg. 1-11

The definitive version is available at:

La versione definitiva è disponibile alla URL:

<http://www.tandfonline.com/doi/full/10.1080/17445647.2015.1077167>

1 **The Meso–Cenozoic stratigraphic succession of the Col de Braus area (Maritime**
2 **Alps, SE France)**

3

4 Luca Barale^{a*}, Anna d’Atri^a, Fabrizio Piana^b

5 a) Dipartimento di Scienze della Terra, Università degli Studi di Torino, Via Valperga

6 Caluso 35 - 10125 Torino, Italy. luca.barale@hotmail.it, anna.datri@unito.it

7 b) Istituto di Geoscienze e Georisorse, Consiglio Nazionale delle Ricerche, Via Valperga

8 Caluso 35 - 10125 Torino, Italy. f.piana@csg.to.cnr.it

9 * Corresponding author.

10

11 **Acknowledgements**

12 The authors thank the Referees Simone Arragoni, Mike Shand, and Thierry Dumont,
13 whose useful suggestions really improved both the manuscript and the geological map.

14 **Abstract**

15 The 1:10,000 geological map here presented extends over about 32 Km² around the Col
16 de Braus pass in the Maritime Alps (SE France). This area attracted the attention of
17 geologists since the late XVIII century due to superb exposures of the Jurassic–
18 Cretaceous Provençal succession, and has become a classic geological locality
19 continuously studied until the present day. In this area, Early Cretaceous synsedimentary
20 tectonics is evidenced by important lateral thickness and facies variations. This sector is
21 presently placed at the western termination of a large structural domain extending from the
22 westernmost Ligurian Alps into the French-Italian Maritime Alps, thus representing a key-
23 area to understand the structural setting of this part of the Western Alps.

24

25 **Keywords:**

26 Provençal Domain; Mesozoic; Nice Arc; Col de Braus; Maritime Alps; SE France

27

28 **1. Introduction and geological setting**

29 The Col de Braus area, in the Nice inland (Maritime Alps, SE France), represents a key-
30 sector for the geology of SE France, as confirmed by the long history of the geological
31 researches that there have been carried out over more than two centuries (see Chapter 3).
32 It corresponds to the southeastern sector of the Alpine External Domain (Dauphinois
33 Domain) that was part, during the Mesozoic, of the European passive margin of the Alpine
34 Tethys. In the Paleogene, the study area became part of the Alpine Foreland Basin that
35 developed in front of the Alpine chain after the first stages of continental collision between
36 Europe and Adria (Crampton & Allen, 1995).

37 The stratigraphic succession unconformably rests on a crystalline basement, currently
38 cropping out in the Argentera Massif, and starts with a thick Upper Carboniferous–Permian
39 continental succession, followed by Lower Triassic siliciclastic coastal deposits, Middle

40 Triassic peritidal carbonates, and Upper Triassic evaporites, related to the early stages of
41 the Alpine Tethys rifting. In the Early Jurassic, the European margin differentiated into a
42 platform domain (Provençal) and a basinal domain (Dauphinois), as a result of extensional
43 tectonics during the Alpine Tethys rifting (Dardeau 1988). In the Provençal Domain, after a
44 period of emersion which included most of the Early Jurassic, Middle–Late Jurassic
45 sedimentation occurred in a carbonate platform environment (Lanteaume, 1968).
46 Valanginian tectonics resulted in the drowning of the carbonate platform (Debelmas &
47 Kerckhove 1980), followed by the deposition, in the study area, of Hauterivian–lower
48 Cenomanian *p.p.* condensed, open-marine shelfal deposits, showing important lateral
49 variations related to synsedimentary tectonics (Pasquini, Lualdi, & Vercesi, 2004; Decarlis
50 & Lualdi 2008). After shelf drowning in the early Cenomanian, a thick hemipelagic
51 succession deposited (early Cenomanian *p.p.*–Campanian). The top of the Mesozoic
52 succession is truncated by a regional unconformity corresponding to a latest Cretaceous–
53 middle Eocene hiatus. Above, the Alpine Foreland Basin succession starts with laterally
54 discontinuous continental to coastal deposits (*Microcodium* Formation, Faure-Muret &
55 Fallot 1954), followed by the middle Eocene ramp Nummulitic Limestone, the hemipelagic
56 upper Eocene *Globigerina* Marl and the upper Eocene–lower Oligocene Grès d’Annot
57 turbidite succession (Ford, Lickhorish, & Kuznir, 1999; Sinclair, 1997).

58 The map area is located at the transition between two structural domains, the Nice Arc and
59 the Roya Arc (Bulard *et al.*, 1975; Gèze, 1963; Perez, 1975) showing different trends of
60 major folds and thrusts (see structural scheme in the Map). The Nice Arc shows variably
61 orientated folds and thrusts, trending NNW-SSE in the western part and E-W to NE-SW in
62 the southern and southeastern part (Bulard *et al.*, 1975; Gèze, 1963; Perez, 1975). The
63 Roya Arc is the westernmost part of a larger structural domain (Roya–Argentina Unit;
64 Piana *et al.*, 2014; d’Atri, Piana, Barale, Bertok, & Martire, in press), extending from the
65 westernmost Ligurian Alps (Nervia–upper Argentina valleys) to the eastern part of the

66 Maritime Alps and bounded toward the north by the Argentera Massif. This domain,
67 showing NNW–SSE to N–S fold trends, has been the target of detailed geological survey
68 in the last 15 years by a research group of the Italian National Research Council (Istituto di
69 Geoscienze e Georisorse) and Torino University (Earth Science Department). The related
70 results have been only partly published (Piana et al., 2014; d’Atri et al., in press). The Col
71 de Braus area is located at the western termination of this domain and will be therefore
72 important in the definition of its western boundary, which is possibly identifiable in the
73 Rocca Serra–Ongrand Thrust (ROT; Guardia, Ivaldi, Dubar, Guglielmi, & Perez, 1996).
74 The map is focused on a small area surrounding the Col de Braus pass, which was
75 previously mapped in the Menton–Nice sheet of the Geological Map of France at 1:50,000
76 (Gèze, Lanteaume, Peyre, & Vernet, 1968). The large representation scale of the
77 presented map (1:10,000) allowed detailed mapping of geological features, in particular:
78 - the lateral variations of Lower Cretaceous lithostratigraphic units, particularly significant
79 in this area;
80 - the distribution of laterally discontinuous continental deposits at the base of the Alpine
81 Foreland Basin succession (*Microcodium* Formation), which were not represented in
82 previous maps; and
83 - the sites with the newly recognized cold-water colonial corals at the top of the Nummulitic
84 Limestone.

85 86 **2. Geohistorical and scientific significance of the Col de Braus area**

87 On the western side of the Col de Braus, the Jurassic–Cretaceous Provençal succession
88 and the lower part of the Eocene Alpine Foreland Basin succession are continuously
89 exposed in a natural stratigraphic section over a thickness of about 1200 m (Figure 1(a),
90 (b)). This section has been firstly mentioned during the late 18th–early 19th century
91 (Beaumont, 1795; Buckland, 1829; Omalius d’Halloy, 1810; Perez, 1847; Risso, 1826;

92 Sismonda, 1848; Sulzer, 1780), and has soon become a “classic” locality for the geology
93 of the Maritime Alps (e.g., Boussac, 1912; Caméré, 1877; Demay, 1984; Fallot, 1885;
94 Gignoux & Moret, 1937; Hébert, 1877; Kilian & Reboul, 1908; Lanteaume, 1968; Potier,
95 1877). In the past decade, detailed stratigraphic and sedimentological analyses have
96 focused on glaucony- and phosphate-rich Lower Cretaceous condensed deposits (Barale,
97 d’Atri and Martire, 2013; Decarlis & Lualdi, 2008; Pasquini et al., 2004, and discussion by
98 Parize *et al.*, 2005; Pasquini and Vercesi, 1999). Different paleontological studies have
99 been dedicated to the fossil-rich Barremian deposits cropping out near Saint Laurent (Bert
100 and Delanoy, 2000; Bert *et al.*, 2006; Delanoy, 1990, 1992; Delanoy, Magnin, Selebran, &
101 Selebran, 1991). The Upper Cretaceous succession of the Col de Braus section was also
102 the subject of detailed biostratigraphic analyses of planktonic foraminifera and calcareous
103 nannofossils (Conard, 1978; Conard & Manivit, 1979), palynofacies (Götz, Feist-Burkhardt,
104 & Ruckwied, 2008), and ammonites (Thomel, 1992).

105

106 **3. Methods**

107 The geological map is drawn at 1:10,000 scale and covers an area of approximately 32
108 km². Data were collected through original fieldwork, stored in a GIS database (Coordinate
109 system: NTF (Paris)/Lambert zone II extended) and represented on a vector topographic
110 map, which has been completely redrawn on the SCAN 25[®] EDR map (1:25,000 scale) of
111 the French National Geographic Institute (IGN).

112 Names of lithostratigraphic units already existing in the literature have been utilized (Alpine
113 Foreland Basin units, and the Grès Verts of the Cretaceous succession). The other
114 Cretaceous units, for which no names existed in the literature, have been newly named
115 after study area localities. Jurassic units have been not renamed, due to their limited
116 extension in the study area, and are referred to using a lithological term preceded by their
117 age (e.g., Callovian dolostones).

118

119 **4. Structural setting**

120 The main structural feature of the mapped area is the SW-vergent Rocca Serra–Ongrand
121 Thrust (ROT; Guardia *et al.*, 1996) also known as Rocca Serra–Touët de l’Escarène
122 Thrust (Bulard *et al.*, 1975). This is a NW–SE-striking, low-angle reverse fault,
123 characterized by a metre-thick shear zone with intense cataclastic deformation, which in
124 the study area runs almost entirely within the Upper Cretaceous succession and has
125 scarce morphological evidence. The ROT crosses the whole map area, dividing it in two
126 structural domains. Its footwall domain is deformed by hectometre- to kilometre-scale,
127 NNW–SSE trending, WSW-vergent open to tight flexural folds, involving the Upper
128 Cretaceous and the Alpine Foreland Basin successions (l’Escarène and Mortisson
129 synclines, l’Escarène anticline), with highly inclined axial surfaces and axes gently
130 plunging toward SSE. The ROT hangingwall domain is instead characterized by a
131 kilometre-scale, NNW–SSE trending open syncline (Col de Braus syncline), affecting the
132 Jurassic-Cretaceous and the Alpine Foreland Basin successions on both sides of the Col
133 de Braus.

134 On the western limb of this syncline, just above the ROT, the Jurassic-Lower Cretaceous
135 succession is involved in a complex structure, known in the literature as “*Écaille*
136 *intercutanée de la Graye de Touët*” [Graye de Touët intracutaneous wedge] (Gèze, 1963).
137 This is a non-cylindrical structure, whose overall N170 strike is oblique to the strike of the
138 ROT. In its middle part (Ruisseau de Redebras valley), it is represented by a kilometre-
139 scale fault-propagation fold affecting the Upper Cretaceous succession and related to the
140 propagation of a blind thrust (Touët de l’Escarène Thrust, TET; section C–C’ in the Map)
141 that causes the local superposition of the Jurassic succession of the Cime de la Graye
142 onto the Upper Cretaceous succession cropping out near Touët de l’Escarène. The latter
143 is characterized by development of drag fold sequences, kinematically consistent with the

144 TET sense of shearing (Figure 2(a)). Toward the north (Roccaniera), the TET evolves as a
145 faulted anticline with a highly inclined axial surface and hectometre-scale slices of
146 Jurassic-Lower Cretaceous succession in its core (see section A–A' in the Map), whereas
147 toward the south it merges in the ROT.

148

149 **5. Stratigraphy**

150 The description of lithostratigraphic units focuses on easily observable field characters, i.e.
151 lithology and macrofossil content. References given beside unit names refer to the age
152 attribution, whereas unit descriptions, if not otherwise specified, are based on original data
153 fully reported in Barale (2010).

154

155 **5.1. Jurassic succession**

156 It consists of a 300-metres-thick carbonate platform succession, mainly cropping out in the
157 Ruisseau de Redebraus valley, downstream of Saint Laurent.

158

159 *5.1.1. Middle Jurassic limestones (Bajocian–Bathonian; Gèze et al., 1968)*

160 Medium- to thick-bedded limestones (packstones/grainstones and rudstones with oncoids,
161 ooids, bioclasts and intraclasts), locally showing a selective dolomitization of the matrix
162 (Figure 2(b)), alternating with medium- to coarsely-crystalline dolostone beds (shallow-
163 water carbonate platform deposits). In the study area, only the uppermost part of this unit
164 crops out (about 20 m thick, referred to the Bathonian; Decarlis, 2005), due to its basal
165 truncation by the TET.

166

167 *5.1.2. Callovian dolostones (Callovian; Dardeau, 1983)*

168 Light brown to beige, medium- to coarsely-crystalline dolostones (locally sucrosic), in
169 decimetre-thick beds; no fossils or internal structures are preserved (carbonate platform

170 deposits). This unit, about 80 m thick, is cut at the top by an unconformity which
171 corresponds to a hiatus spanning the latest Callovian–early Oxfordian (Dardeau & Thierry,
172 1976).

173

174 *5.1.3. Oxfordian limestones (middle–late Oxfordian; Dardeau & Thierry, 1976)*

175 Brown to dark grey, thin- to medium-bedded limestones (bioclastic mudstones to
176 wackestones and minor bioclastic packstones), with belemnites, crinoids, bivalves,
177 gastropods, ammonites, solitary corals, and benthonic foraminifera (outer open-platform
178 deposits). Thickness: 40–50 m.

179

180 *5.1.4. Kimmeridgian limestones (Kimmeridgian–Tithonian p.p.; Dardeau & Thierry, 1976)*

181 Light brown, massive limestones (bioclastic wackestones to packstones and grainstones,
182 bioclastic rudstones), showing a grey colour on weathered surfaces. Abundant reddish-
183 brown chert nodules, disposed in decimetre-spaced layers, give the rock a bedded
184 appearance. Open-platform deposits. Thickness: 70–80 m.

185

186 *5.1.5. Tithonian limestones (Tithonian p.p.–early Berriasian p.p.; Dardeau & Thierry, 1976)*

187 Light-grey massive limestones, consisting of bioclastic–oncoidal–oidal packstones,
188 grainstones and rudstones, locally passing to coral boundstones. The abundant fossil
189 content consists of nerineid gastropods, thick-shelled bivalves, corals, echinoderm
190 fragments, calcareous red and green algae, benthic foraminifera. The uppermost metres
191 are mainly composed of crinoid-rich grainstones. At the top of the unit, a decimetre-thick
192 conglomerate bed with rounded, centimetre-sized reddish intraclasts in a Fe-oxide-rich
193 packstone matrix with millimetre-sized authigenic quartz crystals, is probably referable to
194 an emersion episode. Shallow-water carbonate platform deposits. Thickness: 80 m.

195

196 **5.2. Lower Cretaceous succession**

197 It consists of a peritidal succession (Cime de la Graye Limestone), followed by open-
198 marine shelfal deposits characterized by low sedimentation rates (Grès Verts, Clarissia
199 Formation), and shows important lateral variations (Figure 3) related to synsedimentary
200 tectonics (e.g., Decarlis & Lualdi, 2008; Montenat, Hibsich, Perrier, Pascaud, & de Bretizel,
201 1997; Pasquini et al., 2004). On the eastern side of the Col de Braus ridge (Cime de
202 Ventabren, Vallon du Parais), the thickness of the Cime de la Graye Limestone and the
203 Clarissia Formation is reduced to a few metres each. Therefore, they have been
204 represented as a unique cartographic unit on the map.

205

206 **5.2.1. Cime de la Graye Limestone (early Berriasian p.p.–late Berriasian; Dardeau &**
207 **Pascal, 1982)**

208 Medium- to thick-bedded, light-gray to beige limestones, locally alternating with very thin
209 beds of greenish marls and nodular mudstones with a greenish marly matrix. Limestone
210 beds commonly have an erosional base and show the following internal lithofacies
211 organization (shallowing-upward peritidal cycles; e.g., Wilson, 1975): bioclastic
212 packstones/rudstones (2–10 cm); bioturbated, peloidal–bioclastic mudstones/wackestones
213 (20–100 cm); laminated mudstones with fenestral porosity, millimetre-sized black pebbles,
214 and mud cracks (Figure 2(c)), locally passing to flat-pebble breccias (10–40 cm).
215 Decimetre-thick beds of bioclastic wackestones/packstones with *Clypeina jurassica* and
216 miliolids are locally present (lagoonal sediments; Figure 2(d)). Thickness: 4–25 m.

217

218 **5.2.2. Clarissia Formation (early Hauterivian p.p.–early Aptian p.p.; Barale, 2010; Delanoy,**
219 **1992)**

220 This unit rests on a mineralized hard ground (HG1) developed on top of the underlying
221 Cime de la Graye Limestone. The hard ground, locally encrusted by serpulids and

222 ferruginous microstromatolites (Figure 2(e)), is covered by a centimetre-thick lag deposit
223 made up of mineralized intraclasts and bioclasts (*Hypophylloceras ponticuli*, *Cymatoceras*
224 sp., belemnites). Above, a thin stratigraphic interval (0–1 m), rich in mixed Fe-oxide–
225 phosphate ooids is locally present (Barale *et al.*, 2013). This interval is made up of
226 bioturbated ooidal wackestones/packstones (Figure 2(f)), with reworked cephalopods
227 (*Acanthodiscus* sp., *Lytoceras* sp., Phylloceratidae, *Cymatoceras* sp.), belemnites
228 (*Duvalia* sp.), echinoderms, brachiopods, bivalves, and fish teeth. It is followed by
229 medium-bedded glauconitic limestones (Figure 4(a)) and marly limestones, with *Duvalia*
230 sp., *Cruasiceras cruasense* (Figure 5(a)), *Crioceratites* sp., *Cymatoceras* sp., passing
231 upward to thin-bedded bioclastic mudstones and wackestones, with centimetre-thick marly
232 interbeds, containing *Crioceratites* sp. (Figure 4(b)), *Toxaster* sp., and belemnites (4–20
233 m). At the top of this interval, a mineralized hard ground is present (HG2).

234 In the northwestern sector (Clarissia, Roccaniera), HG2 is followed by a condensed
235 interval made up of glauconitic–phosphatic limestones (120–140 cm, with *Moutoniceras*
236 sp. and belemnites), bioclastic–lithoclastic conglomerates (50–60 cm), and glauconitic
237 limestones (50–60 cm). The conglomerates are made up of reworked bioclasts and
238 centimetre-sized, angular to subrounded limestone intraclasts, commonly phosphatized or
239 impregnated by Fe-oxydes. The reworked bioclasts include ammonites (*Barremites*
240 *difficilis*, *Macroscaphites* sp., *Hypophylloceras ponticuli*, *Pseudohaploceras matheroni*,
241 *Pachyhemihoplites contei*, *P. dardeauai*, *Martelites* sp., *Gassendiceras alpinum*, *Peirescites*
242 sp., *Heinzia sayni*, *Gerhardtia provincialis*, *G.* sp., *Coronites darsi*, *Kotetishvilia*
243 *sauvageai*, *Hemihoplites feraudianus*, *H. astarte*, *H. soulieri*, *H.* sp., *Emericiceras* sp.,
244 *Imerites giraudi*, *Heteroceras baylei*, *H. emerici*, *Argvethites* sp., *Audoliceras* sp.,
245 *Camereiceras* sp., *Lytoceras* sp.) (Figure 5(b–f)), belemnites, nautiloids (*Cymatoceras*
246 sp.), brachiopods, gastropods, bryozoans, and wood fragments. This interval shows
247 important lateral variations: at Saint Laurent it is represented by a 40–50-cm-thick

248 bioclastic–lithoclastic conglomerate bed, followed by a 15–20-cm-thick bed of glauconitic
249 limestone; in the eastern and southern sectors (Albaretta, Vallon du Parais) it reduces to a
250 centimetre-thick bioclastic–lithoclastic lag resting on HG2.

251

252 5.2.3. *Grès Verts* (early Aptian p.p.–early Cenomanian p.p.; Thomel & Lanteaume, 1967;
253 Thomel, 1992)

254 In the western sector, this unit starts with a 8–10-metre-thick alternation of glaucony-rich
255 dark marls and marly limestones, with ammonites (*Lithancylus* sp.) and nautiloids
256 (*Paracymatoceras* sp.). At the top of this interval, a mineralized hard ground (HG3) is
257 followed by a decimetre-thick bioclastic–lithoclastic conglomerate bed. In the eastern
258 sector (Vallon du Parais), this interval is not present and the Grès Verts is lying on a
259 polygenic hard ground (HG2+HG3), developed at the top of the Clarissia Formation and
260 followed by a centimetre-thick bioclastic–lithoclastic lag.

261 The rest of the unit is made up of decimetre-thick beds of bioturbated glauconitic marly
262 limestones, with ammonite molds (*Puzosia* sp.) and echinoids, associated with thick-
263 bedded hybrid glauconitic arenites and glauconarenites, commonly bioturbated, with large-
264 scale cross-stratification (Parize et al., 2005; Pasquini et al., 2004) and decimetre-sized,
265 brownish carbonate concretions (20–40 m). At the top, a decimetre-thick bed of
266 bioturbated, fossil- and glaucony-rich calcareous marl is present. It contains early
267 Cenomanian (*saxbii* Subzone) ammonites (*Mantelliceras picteti* (Figure 5(g)), *M. mantelli*,
268 *M. cantianum*, *M. tuberculatum*, large macroconchs of *Puzosia mayoriana* (Figure 4(c)),
269 *Schloembachia* sp.), echinoids (*Protocardia* sp., *Camerogalerus* sp.), brachiopods,
270 belemnites, bivalves, and lamniform selachian teeth (Figure 4(d)). This bed marks the
271 drowning of the shelf.

272

273 **5.3. Upper Cretaceous succession**

274 It consists of a thick deep water hemipelagic succession of marls and marl–limestone
275 alternations.

276

277 5.3.1. *Saint Laurent Marl* (early Cenomanian p.p.–late Cenomanian; Conard, 1978;
278 Thomel, 1992)

279 Gray, clayey–silty marls, with decimetre-thick marly limestone interbeds whose thickness
280 and frequency increase toward the top of the unit. The fossil content in the lower part of
281 the unit is abundant: ammonites (*Mantelliceras saxbii*, *Schloembachia subvarians*,
282 *Puzosia mayoriana*, *Hypoturritites* sp., *Turrilites costatus*, *Cunningtoniceras cunningtoni*
283 (Figure 5(h)), *Acanthoceras rhotomagense*, *Eucalycoceras* sp., *Calycoceras* sp.,
284 *Newboldiceras* sp., Phylloceratinae), terebratulids, belemnites (*Neohibolites* sp.),
285 echinoids (*Camerogalerus cylindricus*, *Holaster subglobosus*), and bivalves (*Inoceramus*
286 sp.). Thickness: 60–80 m.

287

288 5.3.2. *Mont Auri Limestone* (Turonian–late Coniacian p.p.; Conard & Manivit, 1979)

289 Marly limestones (planktonic-foraminifera mudstones and wackestones) with thin marl
290 interbeds, passing toward the top to medium-bedded limestones (bioclastic wackestones
291 and packstones), with echinoids (*Micraster* sp., *Holaster* sp.) and bivalves (*Inoceramus*
292 sp.). In the upper part, grey-coloured chert nodules, and thin- to medium-bedded
293 resedimented glauconitic lithoarenites and hybrid glauconitic arenites are present. These
294 beds have an erosional base, locally followed by imbricated clay chips or by a centimetre-
295 thick lag consisting of *Inoceramus* fragments, and show normal grading and parallel
296 lamination. Thickness: 300 m.

297

298 5.3.3. *Caire de Braus Marl* (late Coniacian p.p.–middle Campanian; Conard & Manivit,
299 1979)

300 Alternation of medium- to thick-bedded marls and marly limestones (Figure 4(e)),
301 commonly bioturbated (*Zoophycos*), with *Inoceramus* sp., echinoids, planktonic
302 foraminifera and rare ammonite molds. In the uppermost 100 metres, thin resedimented
303 beds of bioclastic packstones with planktonic foraminifera and glaucony are present,
304 showing erosional base, normal grading and parallel lamination. Thickness: 350 m.

305

306 **5.4. Alpine Foreland Basin Succession**

307 It is represented in the study area by the *Microcodium* Formation, the Nummulitic
308 Limestone and the *Globigerina* Marl, cropping out in the core of the Col de Braus,
309 l'Escarène and Mortisson synclines.

310

311 5.4.1. *Microcodium* Formation (Lutetian? –early Bartonian; Varrone & Clari, 2003)

312 Lenticular bodies, 0–15-m thick, including from base to top the following, laterally
313 discontinuous, facies and facies associations:

314 - polygenic, clast-supported conglomerates, with marly limestone and limestone clasts
315 (locally encrusted by *Microcodium*) mainly derived from the underlying Upper Cretaceous
316 succession, with arenitic or marly matrix with *Microcodium* fragments (S Col de Braus
317 syncline; l'Escarène; Blanchières) (alluvial fan–fluvial deposits);

318 - silty marls, containing decimetre-thick, lens-shaped bodies of clast-supported
319 conglomerates and decimetre-thick beds of quartz-rich arenites with reworked glaucony
320 grains (NE l'Escarène syncline; Mont Brec) (alluvial plain sediments with channelized
321 fluvial deposits);

322 - medium- to coarse-grained, thick-bedded quartzarenites, with erosional base, clay chips,
323 and trough cross-stratification, locally containing centimetre-thick conglomerate beds (SW
324 Col de Braus syncline). *Ophiomorpha* burrows are locally preserved as hypichnia at the
325 base of this interval (coastal deposits).

326 The *Microcodium* Formation unit represents the infilling of an incised valley system during
327 the first stage of the Alpine Foreland Basin development (Varrone & Clari, 2003).

328

329 5.4.2. *Nummulitic Limestone (Bartonian p.p.; Varrone & Clari, 2003)*

330 This unit consists of mixed siliciclastic-carbonate ramp deposits. Its base is represented
331 by a transgressive erosional surface, locally covered by a centimetre- to decimetre-thick
332 conglomerate lag and developed on the *Microcodium* Formation or directly on top of the
333 Upper Cretaceous succession. In the latter case, it consists of a polygenic discontinuity
334 surface, pitted by abundant *Gastrochænoletes* bivalve borings (Figure 4(f)). From base to
335 top, the following facies and facies associations are present:

336 - thick- to very thick-bedded, medium- to coarse-grained quartzarenites showing an
337 erosional base and normal gradation, grading upward to medium- to fine-grained
338 bioclastic–lithic arenites, with larger benthic foraminifera (*Nummulites*), ostreids, echinoids
339 and rare solitary corals (inner- to middle-ramp deposits);

340 - medium-bedded, medium- to fine-grained allochemic sandstones and siltstones, with
341 *Nummulites*, bivalves, gastropods, solitary corals, echinoids, scaphopods, and *Teredolites*-
342 bored wood fragments, passing upward to an alternation of intensely bioturbated, fine-
343 grained allochemic sandstones and calcareous marls (outer ramp deposits).

344 In the Col de Braus syncline, the top of the unit is represented by a decimetre-thick interval
345 of fine-grained, glaucony-bearing hybrid arenite, locally containing cold-water colonial
346 corals (whose study is currently in progress). This interval marks the drowning of the ramp.

347

348 5.4.3. *Globigerina Marl (late Bartonian p.p.–Priabonian; Varrone, 2004)*

349 Dark-grey deep water hemipelagic silty marls, light-gray to yellowish on the weathered
350 surface, with abundant planktonic foraminifera and rare bivalves, showing centimetre- to
351 decimetre-thick bedding, commonly obliterated by intense bioturbation.

352

353 **5.5. Quaternary deposits**

354 The detailed study of Quaternary deposits is out of the scope of this work, therefore they
355 will be only listed as they appear on the map. They have been subdivided into five large
356 groups: anthropic deposits; undifferentiated alluvial deposits; slope and talus debris;
357 cemented talus breccias; landslide accumulations.

358

359 **6. Lucéram arsenic mine**

360 At Roccaniera, near Lucéram, an arsenic mineralization was exploited during the XIX–
361 early XX centuries (Caméré, 1877; Lacroix, 1897; Orcel, 1918). The mineralization affects
362 the Grès Verts and the lower part of the Saint Laurent Marl and consists of decimetre-
363 thick, nearly bed-parallel veins, filled-up by calcite, orpiment, realgar, barite and fluorite
364 (Féraud, 1970). It also yielded specimens of talmessite, a rare arsenate mineral (Mari &
365 Mari, 1982).

366

367 **7. Conclusions**

368 The 1:10,000 Geological Map of the Col de Braus area gives a detailed representation of a
369 sector of great scientific relevance, which also represents a historical locality for SE
370 France geology. This map constitutes a useful complementary document to address
371 specific features regarding both stratigraphic and structural issues of lively geological
372 interest, namely:

373 - the stratigraphy and sedimentology of Lower Cretaceous condensed deposits, which
374 have been the focus of various publications in the last years (e.g., Barale *et al.*, 2013;
375 Decarlis & Lualdi, 2008; Pasquini *et al.*, 2004);

376 - the distribution of laterally discontinuous continental deposits at the base of the Eocene
377 Alpine Foreland Basin succession (*Microcodium* Formation), as well as the position of the

378 outcrops with newly-reported colonial cold-water corals at the top of the Nummulitic
379 Limestone;
380 - the structural setting of an area located at the western termination of a large structural
381 domain, extending across the Ligurian and the Maritime Alps, which has been the object of
382 a pluriannual detailed work of structural and stratigraphic analysis.

383

384 **Software**

385 The compilation of the geological map, including the preparation of the topographic base,
386 was done using QuantumGis 2.0 Dufour. The final layout of the map, the geologic
387 sections, the tectonic sketch map, and the figures have been prepared and assembled
388 using ACD® Canvas12.

389

390

391 **References**

392 Barale, L. (2010). *La successione giurassico–cretacica del Dominio Delfinese-Provenzale*
393 *(Col de Braus, Francia)* (Unpublished master's thesis). Torino: Università di Torino.

394 Barale, L., d'Atri, A., & Martire, L. (2013). The role of microbial activity in the generation of
395 Lower Cretaceous mixed Fe-oxide–phosphate ooids from the Provençal Domain,
396 French Maritime Alps. *J. Sed. Res.*, 83, 196–206. doi: [10.2110/jsr.2013.15](https://doi.org/10.2110/jsr.2013.15)

397 Beaumont, A. (1795). *Travels through the Maritime Alps, from Italy to Lyons, across the*
398 *Col de Tende, by the way of Nice, Provence, Languedoc, &c. with topographical and*
399 *historical descriptions*. London: Bensley.

400 Bert, D., & Delanoy, G. (2000). Considérations nouvelles sur quelques représentants
401 barrémiens des Pulchellidae DOUVILLÉ, 1890 et des Hemihoplitidae SPATH, 1924
402 (Ammonoidea) [New considerations about some Barremian representatives of the

403 Pulchellidae DOUVILLÉ, 1890 and of the Hemihoplitidae SPATH, 1924 (Ammonoidea)].
404 *Ann. Mus. Hist. Nat. Nice*, 15, 63–89.

405 Bert, D., Delanoy, G., & Bersac, S. (2006). Descriptions de représentants nouveaux ou
406 peu connus de la famille des Hemihoplitidae SPATH, 1924 (Barrémien supérieur, Sud-
407 est de la France): conséquences taxinomiques et phylétiques [Descriptions of new or
408 poorly known representatives of the family Hemihoplitidae SPATH, 1924 (late
409 Barremian, SE of France): taxonomic and phyletic consequences]. *Ann. Mus. Hist. Nat.*
410 *Nice*, 21, 179–253.

411 Boussac, J. (1912). *Études stratigraphiques sur le Nummulitique alpin* [Stratigraphic
412 studies on the Alpine Nummulitic]. Paris: Mem. Serv. Carte Géol. Fr.

413 Buckland, W. (1829). Observations on the Secondary Formations between Nice and the
414 Col di Tendi. *Trans. Geol. Soc. London*, 3, 187–190.

415 Bulard, P.F., Chamagne, B., Dardeau, G., Delteil, J., Gioan, P., Ivaldi, J.P., ... Polvêche, J.
416 (1975). Sur la genèse des structures de l'Arc de Nice [On the genesis of the structures
417 of the Nice Arc]. *Bull. Soc. Géol. Fr. (7)*, 17, 939–944.

418 Caméré, M. (1877). Note sur la Carte géologique d'une portion du département des Alpes-
419 Maritimes [Note on the Geological Map of a part of the Alpes-Maritimes department]. *Bull.*
420 *Soc. Géol. Fr. (3)*, 5, 803–808.

421 Conard, M. (1978). Le Cénomaniens des Alpes-Maritimes: biozonation par les
422 Globotruncanidés [The Cenomanian of the Maritime Alps: Globotruncanid biozonation].
423 *Géologie Méditerranéenne*, 5 (1), 65–68.

424 Conard, M., & Manivit, H. (1979). Contribution à l'étude biostratigraphique du Crétacé
425 supérieur d'une coupe du Massif du Braus (Alpes-Maritimes, SE France) [Contribution
426 to the biostratigraphic study of a section of the Braus Massif (Maritime Alps, SE
427 France)]. *Géobios*, 12, 437–443.

- 428 Crampton, S.L., & Allen, P.A. (1995). Recognition of forebulge unconformities associated
429 with early stage foreland basin development: example from the North Alpine Foreland
430 Basin. *AAPG Bulletin*, 79, 1495–1514.
- 431 Dardeau G. (1983) – Le jurassique des Alpes-Maritimes (France). Stratigraphie,
432 paléogéographie, evolution du context structural à la junction des dispositifs dauphinois,
433 briançonnais et provençal. (Unpublished doctoral thesis). Nice: Université de Nice.
- 434 Dardeau, G. (1988). Tethyan evolution and Alpine reactivation of Jurassic extensional
435 structures in the French “Alpes maritimes”. *Bull. Soc. Géol. Fr.* (8), 4, 651–657.
- 436 Dardeau, G., & Thierry J. (1976). Discontinuité de sédimentation et biostratigraphie a la
437 base du Jurassique supérieur de la partie méridionale de l'Arc de Nice, entre La Turbie
438 et Eze (Alpes-Maritimes) [Sedimentation discontinuity and biostratigraphy at the base of
439 the Upper Jurassic of the southern Nice Arc, between La Turbie and Eze (Maritime
440 Alps)]. *Bull. Soc. Géol. Fr.* (7), 18, 1631–1635.
- 441 Dardeau, G., & Pascal, A. (1982). La regression fin-Jurassique dans les Alpes-Maritimes:
442 Stratigraphie, faciès, environnements sédimentaires et influence du bâti structural dans
443 l'Arc de Nice [The end-Jurassic regression in the Maritime Alps: Stratigraphy, facies,
444 sedimentary environments and influence of the structural setting in the Nice Arc].
445 *Bulletin du B.R.G.M.*, 3, 193–204.
- 446 d'Atri, A., Piana, F., Barale, L., Bertok, C., & Martire, L. (in press) Geological setting of the
447 southern termination of Western Alps. *Int. Journ. of Earth Sci.*
- 448 Debelmas, J., & Kerckhove, C. (1980). Les Alpes franco-italiennes [The French–Italian
449 Maritime Alps]. *Géol. Alp.*, 56, 21–58.
- 450 Decarlis, A. (2005). *Fasi deposizionali terminali delle piattaforme carbonatiche*
451 *mesozoiche delfinesi-provenzali (arco di Nizza)* (Unpublished doctoral dissertation).
452 Pavia: Università di Pavia.

453 Decarlis, A., & Lualdi, A. (2008). Stratigraphy and deposition of Lower Cretaceous
454 condensed deposits in the Maritime Alps (Nice arc, SE France). *Ital J. Geosci.*, 127, 13–
455 24.

456 Delanoy, G. (1990). *Camereiceras nov. gen.* (Ammonoidea, Ancyloceratina) du Barrémien
457 supérieur du Sud-Est de la France [*Camereiceras nov. gen.* (Ammonoidea,
458 Ancyloceratina) of the late Barremian of the SE France]. *Geobios*, 23, 71–93.

459 Delanoy, G. (1992). Les ammonites du Barrémien supérieur de Saint-Laurent de
460 l'Escarène (Alpes-Maritimes, Sud-Est France) [Late Barremian ammonites of Saint-
461 Laurent de l'Escarène (Maritime alps, SE France)]. *Ann. Mus. Hist. Nat. Nice*, 9, 1–148.

462 Delanoy, G., Magnin, A., Selebran, M., & Selebran, J. (1991). *Moutoniceras nodosum*
463 D'ORBIGNY, 1850 (Ammonoidea, Ancyloceratina). Une très grande ammonite
464 hétéromorphe du Barrémien inférieur [*Moutoniceras nodosum* D'ORBIGNY, 1850
465 (Ammonoidea, Ancyloceratina). A very large heteromorphic ammonite of the early
466 Barremian]. *Revue de Paléobiologie*, 10, 229–245.

467 Demay, J.-L. (1984). Alpes Méridionales [Southern Alps]. In S. Debrand-Passard, S.
468 Courbouleix, & M.J. Lienhardt (Eds.), *Synthèse géologique du Sud-Est de la France*,
469 125, 317–319.

470 Fallot, E. (1885). Etude géologique sur les étages moyen et supérieur du terrain crétacé
471 dans le SE de la France [Geological study on the Middle and Upper Cretaceous
472 succession in the SE of France]. *Ann. Sc. Geol.*, 18, 1–268.

473 Faure-Muret, A., & Fallot, P. (1954). Sur le Secondaire et le Tertiaire aux abords sud-
474 orientaux du massif de l'Argentera-Mercantour [On the Secondary and Tertiary
475 successions at the southeastern edge of the Argentera–Mercantour Massif]. *Bull. Serv.*
476 *Carte Géol. France*, 241, 189–198.

477 Féraud, J. (1970). *Les gisements de sulfures d'arsenic des Alpes Maritimes et de la Corse*
478 (Public Report No. RME-041-RMM). Orléans: BRGM.

479 Ford, M., Lickhorish, W.H., & Kuznir, N.J. (1999). Tertiary Foreland sedimentation in the
480 Southern Subalpine Chains, SE France: a geodynamics appraisal. *Basin Res.*, 11, 315–
481 336. doi: [10.1046/j.1365-2117.1999.00103.x](https://doi.org/10.1046/j.1365-2117.1999.00103.x)

482 Gèze, B. (1963). Caractères structuraux de l'Arc de Nice (Alpes-Maritimes) [Structural
483 characters of the Nice Arc (Maritime Alps)]. *Mèm. H.S. Soc. Géol. Fr.*, 2, 289–300.

484 Gèze, B., Lanteaume, M., Peyre, Y., & Vernet, J. (1968). Carte Géologique au 1/50000
485 Menton-Nice, XXXVII-42-43. Orléans: BRGM.

486 Gignoux, M., & Moret, L. (1937). Sur l'extension des lagunes purbeckiennes dans le Sud-
487 Est de la France [On the extension of Purbeckian lagoons in SE France]. *C.R. somm.*
488 *Soc. Géol. Fr.*, 116–117.

489 Götz, A. E., Feist-Burkhardt, S., & Ruckwied, K. (2008). Palynofacies and sea-level
490 changes in the Upper Cretaceous of the Vocontian Basin, southeast France.
491 *Cretaceous Res.*, 29, 1047–1057. doi:[10.1016/j.cretres.2008.05.029](https://doi.org/10.1016/j.cretres.2008.05.029)

492 Guardia, P., Ivaldi, J.-P., Dubar, M., Guglielmi, Y., & Perez, J.-L. (1996). Paléotectonique
493 linéamentaire et tectonique active des Alpes Maritimes franco-italiennes: une synthèse
494 [Lineamentar paleotectonics and active tectonics of the French-Italian Maritime Alps: a
495 synthesis]. *Géologie de la France*, 1, 43–55.

496 Hébert, E. (1877). Coupe du terrain crétacé de Saint-Laurent [Stratigraphic section of the
497 Cretaceous succession of Saint-Laurent]. *Bull. Soc. Géol. Fr. (3)*, 5, 810.

498 Kilian, W., & Reboul, P. (1908). Quelques observations géologiques dans la région sud-est
499 des Alpes Maritimes [Some geological observation in the southeastern sector of the
500 Maritime Alps]. *Bull. Serv. Carte Géol. Fr.*, 119, 155–165.

501 Lacroix, A. (1897). *Minéralogie de la France et de ses colonies* [Mineralogy of France and
502 its colonies]. Paris: Librairie Polytechnique, Baudry et C. Éditeurs.

- 503 Lanteaume, M. (1968). *Contribution à l'étude géologique des Alpes Maritimes franco-*
504 *italiennes* [Contribution to the geological study of the French–Italian Maritime Alps].
505 Paris: Mém. Carte Géol. France.
- 506 Mari, D., & Mari, G. (1982). *Mines et minéraux des Alpes Maritimes* [Mines and minerals of
507 the Maritime Alps]. Nice: Serre éditeur.
- 508 Montenat, C., Hibsich, C., Perrier, J.C., Pascaud, F., & de Bretizel, P. (1997). Tectonique
509 cassante d'âge crétacé inférieur dans l'Arc de Nice (Alpes-Maritimes, France) [Early
510 Cretaceous brittle tectonics in the Nice Arc (Maritime Alps, France)]. *Géol. Alp.*, 73, 59–
511 66.
- 512 Orcel, J. (1918). Les gisements d'orpiment et de réalgar de Lucéram et de Duranus
513 (Alpes-Maritimes) [The orpiment and realgar ore deposits of Lucéram and Duranus
514 (Maritime Alps)]. *Bull. Soc. Fr. Minér.*, 41, 176–180.
- 515 Omalius d'Halloy, J.J. (1810). Notice géologique sur la route du Col de Tende, dans les
516 Alpes maritimes, précédée de Considérations sur les terrains intermédiaires [Geological
517 note on the Col de Tende road, in the Maritime Alps, preceded by considerations on the
518 intermediary rocks]. *Journal des Mines*, 28, 169–196.
- 519 Parize, O., Fiet, N., Friès, G., Imbert, P., Latil, J.-L., Rubino, J.-L., & Viana, A. (2005).
520 “Depositional dynamics of glaucony-rich deposits in the Lower Cretaceous of the Nice
521 arc, southeast France” [Cretaceous Research 25 (2004) 179–189] – Discussion.
522 *Cretaceous Res.*, 26, 726–730. [doi:10.1016/j.cretres.2005.05.001](https://doi.org/10.1016/j.cretres.2005.05.001)
- 523 Pasquini, C., Lualdi, A., & Vercesi, P.L. (2004). Depositional dynamics of glaucony-rich
524 deposits in the Lower Cretaceous of the Nice arc, southeast France. *Cretaceous Res.*,
525 25, 179–189. [doi:10.1016/j.cretres.2003.11.005](https://doi.org/10.1016/j.cretres.2003.11.005)
- 526 Pasquini, C., & Vercesi, P.L. (1999). Sedimentazione condensata barremiano-
527 cenomaniana al margine sud-orientale della zona Delfinese-Provenzale [Barremian-

528 Cenomanian condensed sedimentation at the southeastern margin of the Provençal-
529 Dauphinois Domain]. *Giornale di geologia*, 61, 249–251.

530 Perez, A. (1847). Comunicazione sui limiti del terreno cretaceo delle Alpi Marittime
531 [Communication on the limits of the Cretaceous rocks in the Maritime Alps]. In: *Atti della*
532 *ottava riunione degli scienziati italiani* (pp. 651–658). Genova: Tipografia Ferrando.

533 Perez, J.-L. (1975). La zone limite entre l'arc de Nice et l'arc de la Roya (Alpes Maritimes).
534 Observations structurales [The boundary zone between the Nice Arc and the Roya Arc
535 (Maritime Alps). Structural observations]. *Bull. Soc. Géol. Fr.*, 7, 930–938.

536 Piana, F., Battaglia, S., Bertok, C., d'Atri, A., Ellero, A., Leoni, L., ... Perotti, E. (2014). Illite
537 (KI) and chlorite (AI) 'crystallinity' indices as a constraint for the evolution of the External
538 Briançonnais Front in Western Ligurian Alps (NW Italy). *It. J. Geosci.*, 133, 445–454.
539 [doi: 10.3301/IJG.2014.21](https://doi.org/10.3301/IJG.2014.21)

540 Potier (1877). Compte-rendu de la course de L'Escarène et du Col de Braus [Report on
541 the field-trip to L'Escarène and the Col de Braus]. *Bull. Soc. Géol. Fr.* (3), 5, 808–811.

542 Risso, A. (1826). Histoire naturelle des principales productions de l'Europe Méridionale et
543 particulièrement de celles des environs de Nice et des Alpes Maritimes. Tome Premier
544 [Natural history of the main productions of Southern Europe and in particular of those of
545 the surroundings of Nice and of the Maritime Alps. Volume I]. Paris: Levrault.

546 Sinclair, H.D. (1997). Tectonostratigraphic model for underfilled peripheral foreland basins:
547 an Alpine perspective. *GSA Bull.*, 109, 324–346. [doi: 10.1130/0016-](https://doi.org/10.1130/0016-7606(1997)109<0324:TMFUPF>2.3.CO;2)
548 [7606\(1997\)109<0324:TMFUPF>2.3.CO;2](https://doi.org/10.1130/0016-7606(1997)109<0324:TMFUPF>2.3.CO;2)

549 Sismonda, A. (1848). Notizie e chiarimenti sulla costituzione della Alpi piemontesi
550 [Information and explanations about the constitution of the Piedmont Alps]. *Mem. R.*
551 *Accad. Sc. Torino*, 9, 1–123.

552 Sulzer, J.G. (1780). *Tagebuch einer von Berlin nach den mittäglichen Ländern von Europa*
553 *in den Jahren 1775 und 1776 gethanen Reise und Rückreise* [Diary of a round trip from

554 Berlin to the lands of the Southern Europe in the years 1775 and 1776]. Leipzig:
555 Weidmann.

556 Thomel, G. (1992). *Ammonites du Cénomanién et du Turonien du Sud-Est de la France*
557 [Ammonites of the Cenomanian and the Turonian of SE France]. Nice: Serre éditeur.

558 Thomel, G., & Lanteaume, M. (1967). Considérations sur la mise en évidence des dépôts
559 aptiens dans la région niçoise [Considerations about the discovery of Aptian deposits in
560 the Nice area]. *C. R. Acad. Sci. Paris*, 265, 1456–1459.

561 Varrone, D. (2004). *Le prime fasi di evoluzione del bacino di avana fossa alpino: la*
562 *succession delfinese cretacico-eocenica, Alpi Marittime* (Unpublished doctoral
563 dissertation). Università di Torino.

564 Varrone, D., & Clari, P. (2003). Stratigraphic and paleoenvironmental evolution of the
565 *Microcodium* Formation and the Nummulitic Limestones in the French–Italian Maritimes
566 Alps. *Geobios*, 36, 775–786.

567 Wilson, J.L. (1975). Carbonate facies in geologic history. Berlin: Springer–Verlag.

568

569 **Figure captions**

570

571 Figure 1. Panoramic view (a) and explanatory sketch (b) of the Col de Braus stratigraphic
572 succession exposed on the northern side of the Ruisseau de Redebras valley
573 (background); in the foreground, the transition from the Tithonian limestones to the Cime
574 de la Graye Limestone cropping out near Albaretta, on the southern side of the same
575 valley. Image taken from Albaretta locality (43°50'56.3" N; 7°22'37.5" E), looking
576 northwards.

577

578 Figure 2. Field and thin section features of the stratigraphic succession in the Col de Braus
579 area. (a) Chevron drag folds in the marl-limestone alternations (Caire de Braus Marl)

580 in the footwall of the Touët de l'Escarène Thrust, cropping out along the D2204 road near
581 Touët de l'Escarène. (b) Bed of intraclast rudstone in the Middle Jurassic limestones,
582 showing a selective dolomitization of the matrix; Rochers de Saint Sauveur. (c) Bedding
583 surface with mud cracks in the upper part of the Cime de la Graye Limestone; Saint
584 Laurent. (d) Bioclastic packstone rich in *Clypeina jurassica* fragments from the upper part
585 of the Cime de la Graye Limestone; Roccaniera. Thin section photomicrograph, plane-
586 polarized light. (e) Ferruginous microstromatolites hanging from the roof of a small cavity
587 within the mineralized crust (M, mainly made up of Fe-oxyhydroxides) coating the hard
588 ground HG1; Saint Laurent. The cavity is filled-up by a micritic sediment (S), giving rise to
589 a geopetal structure plugged by later calcite cement (C). Thin section photomicrograph,
590 plane-polarized light. (f) Weathered bedding surface of the basal deposits of the Clarissia
591 Formation, showing the ellipsoidal mixed Fe-oxide–phosphate ooids; Cime de la Graye.

592

593 Figure 3. Correlative scheme showing the lateral variations of the Lower Cretaceous
594 succession in the study area (stratigraphic sections: AL, Albaretta; SL, Saint Laurent; RN,
595 Roccaniera; VP, Vallon du Parais). Stratigraphic sections have been aligned in
596 correspondence of the base of the Saint Laurent Marl. Abbreviations of lithostratigraphic
597 units: TIT, Tithonian limestones; GRA, Cime de la Graye Limestone; CLA, Clarissia
598 Formation; GV, Grès Verts (GVa, lower interval; GVb, upper interval); SLM, Saint Laurent
599 Marl.

600

601 Figure 4. Field and thin section features of the stratigraphic succession in the Col de Braus
602 area. (a) Bioturbated, glauconitic bioclastic packstone in the lower part of the Clarissia
603 Formation (Roccaniera), showing brilliant-green glaucony grains and some phosphatic
604 ooids (arrow points); the glaucony-poor portions correspond to burrows. Thin section
605 photomicrograph, plane-polarized light. (b) Bedding surface of a bioclastic wackestone bed

606 in the Clarissia Formation, showing internal (to the left) and external (to the right) moulds
607 of *Crioceratites* sp.; Cime de la Graye. (c) Large macroconch of *Puzosia* sp. in the
608 bioturbated, glaucony-rich calcareous marl at the top of the Grès Verts; Saint Laurent. (d)
609 Lamniform selachian tooth on a weathered surface of the glaucony-rich calcareous marly
610 bed at the top of the Grès Verts (note the dark-green glaucony grains sticking out of the
611 surface); Roccaniera. (e) Alternations of thin-bedded marly limestones and marls in the
612 lower part of the Caire de Braus Marl, cropping out along the D2204 road north of Saint
613 Laurent. (f) Polygenic discontinuity surface separating the Nummulitic Limestone (NL) from
614 the underlying Caire de Braus Marl (CBM), showing abundant *Gastrochaenolites* bivalve
615 borings; Rocher de Pianastan.

616

617 Figure 5. Ammonites from the Cretaceous succession of the Col de Braus area. (a)
618 *Cruasicerias cruasense* (lower part of the Clarissia Formation, eastern side of Cime de la
619 Graye). (b–f) reworked ammonites from the bioclastic–lithoclastic conglomerates in the
620 upper part of the Clarissia Formation, Clarissia (b, *Gassendicerias alpinum*; c,
621 *Hemihoplites feraudianus*; d, *Pachyhemihoplites contei*; e, *Kotetishvilia sauvageaui*; f,
622 *Argvethites* sp.). (g) *Mantelliceras picteti* (top bed of the Grès Verts, Saint Laurent). (h)
623 *Cunningtoniceras cunningtoni* (Saint Laurent Marl, Villatalla). Scale bars: a–b, 5 cm; c–h, 1
624 cm. Arrows in (a), (d), (e), and (f) point to the last septal suture.

625

626

627

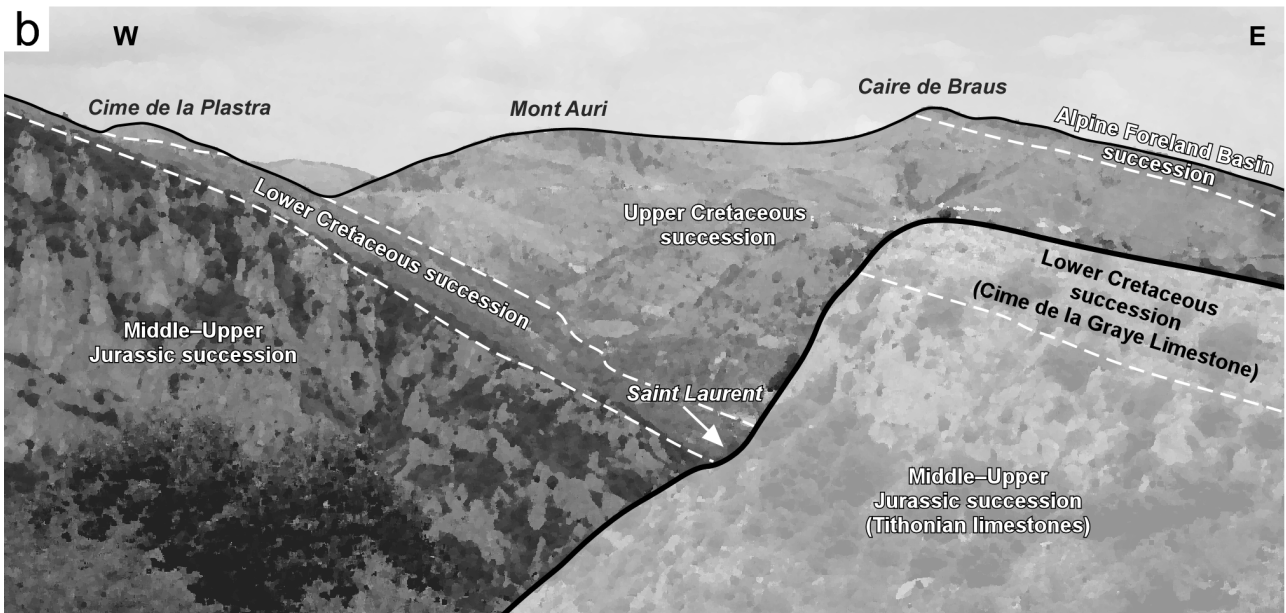
628

629

630

631

632 Figure 1



634

635

636

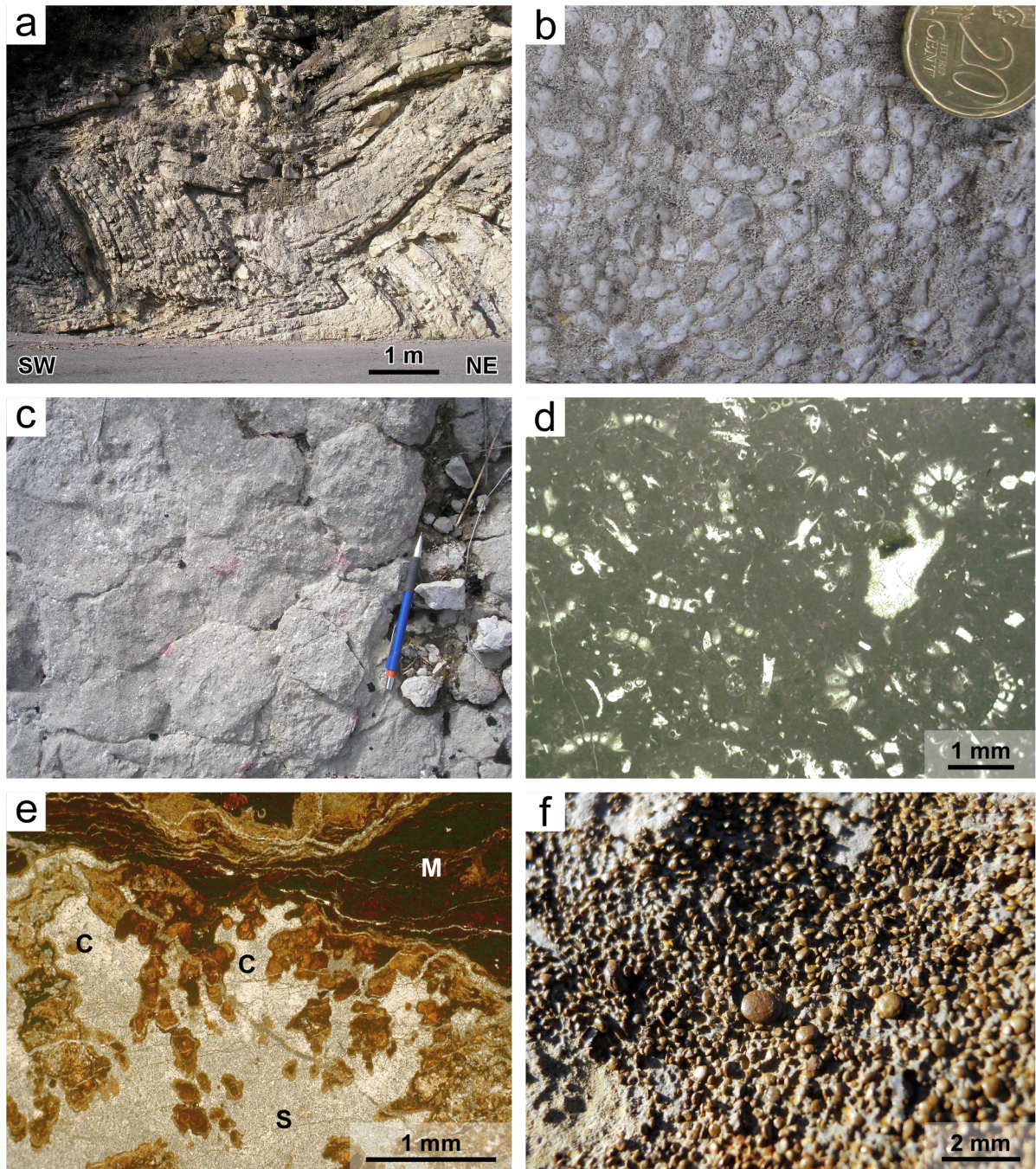
637

638

639

640

641 Figure 2



643

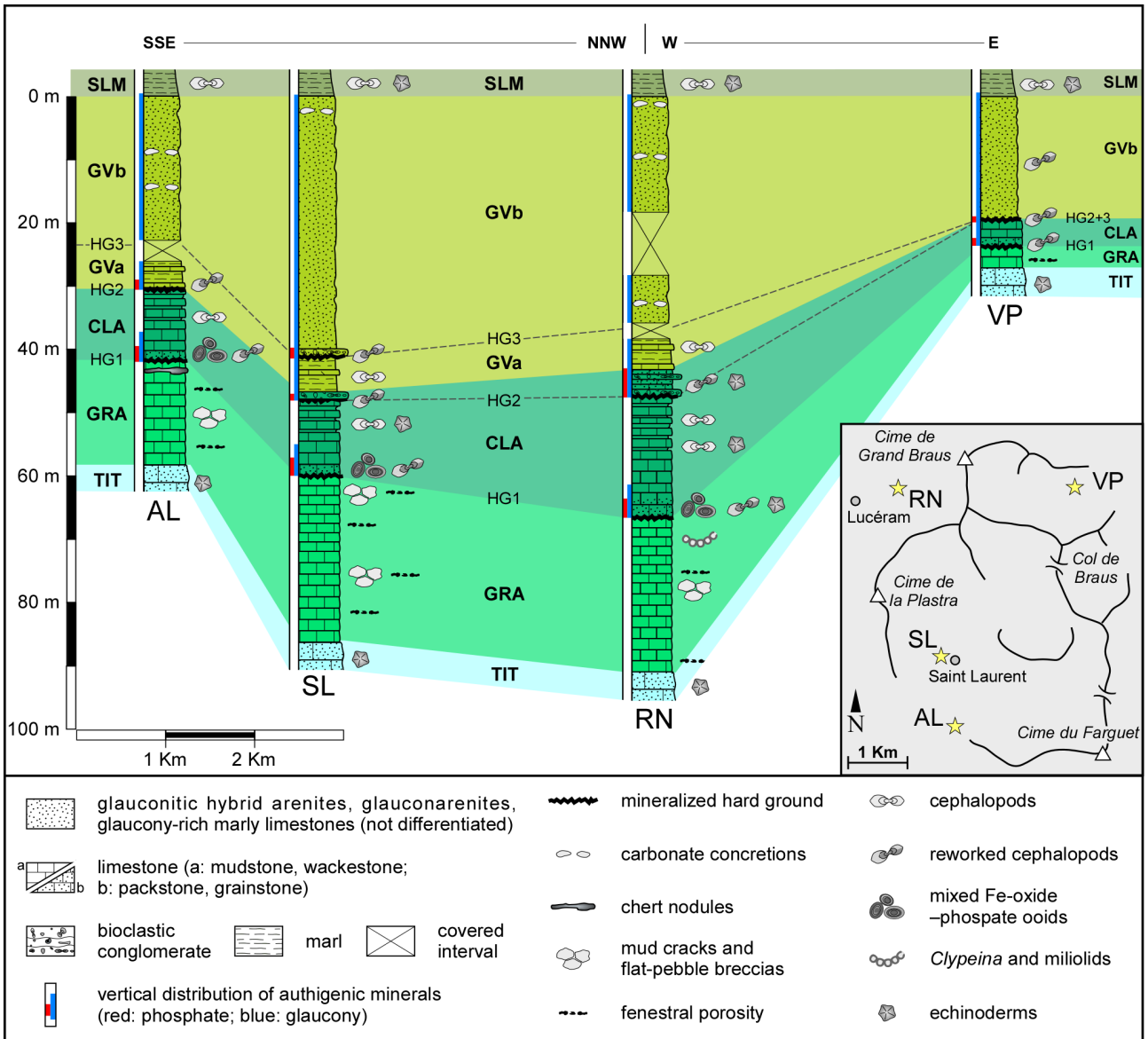
644

645

646

647

648 Figure 3



650

651

652

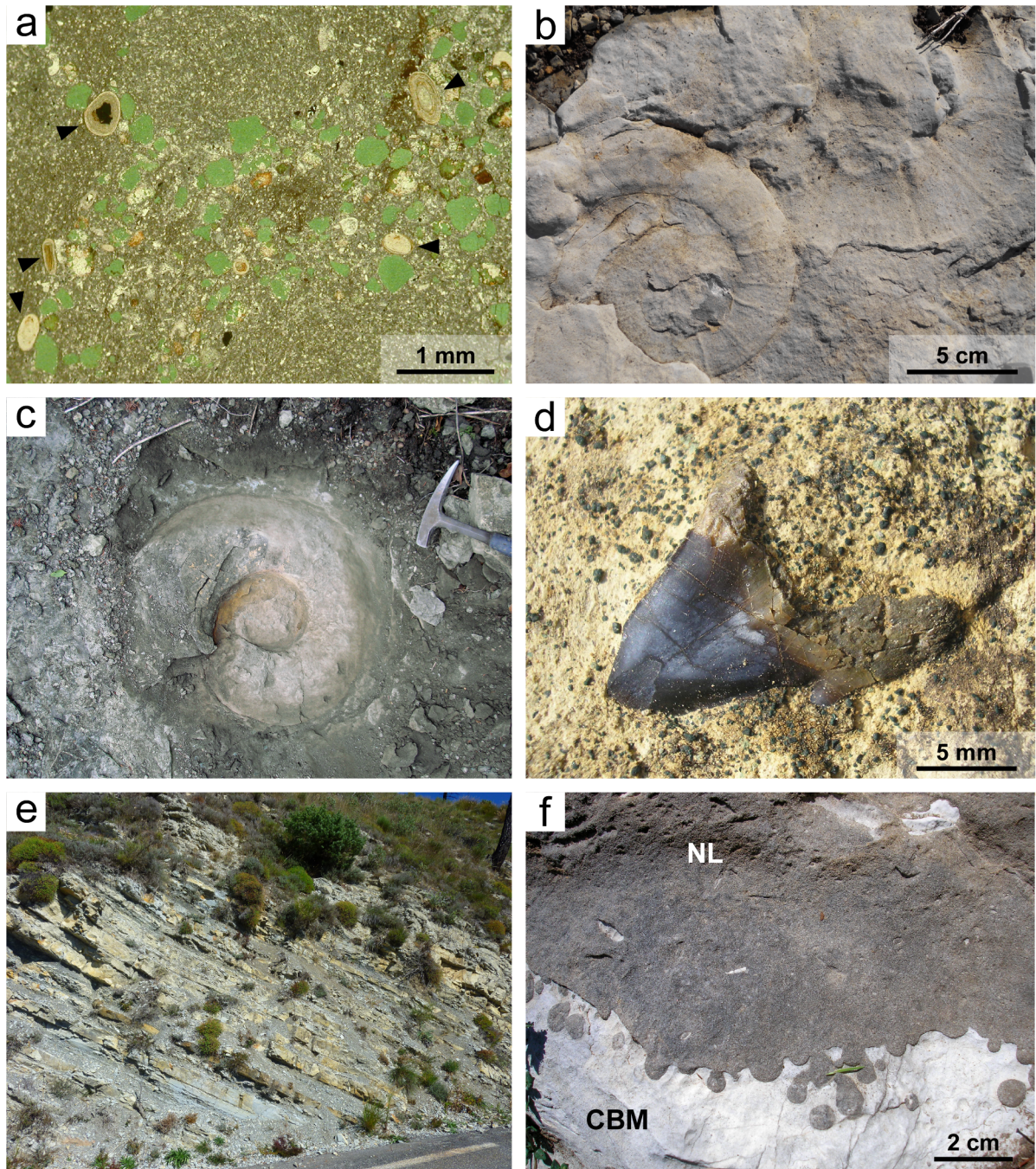
653

654

655

656

657



660

661

662

663

664

